# Heat-to-Heat Variation in Creep Life and Fundamental Creep Rupture Strength of 18Cr-8Ni, 18Cr-12Ni-Mo, 18Cr-10Ni-Ti, and 18Cr-12Ni-Nb Stainless Steels

FUJIO ABE

Metallurgical factors causing the heat-to-heat variation in time to rupture have been investigated for 300 series stainless steels for boiler and heat exchanger seamless tubes, 18Cr-8Ni (JIS SUS 304HTB), 18Cr-12Ni-Mo (JIS SUS 316HTB), 18Cr-10Ni-Ti (JIS SUS321 HTB), and 18Cr-12Ni-Nb (JIS SUS 347HTB), at 873 K to 1023 K (600 °C to 750 °C) using creep rupture data for nine heats of the respective steels in the NIMS Creep Data Sheets. The maximum time to rupture was 222,705.3 hours. The heat-to-heat variation in time to rupture of the 304HTB and 316HTB becomes more significant with longer test durations at times above ~10,000 hours at 973 K (700 °C) and reaches to about an order of magnitude difference between the strongest and weakest heats at 100,000 hours, whereas that of the 321HTB and 347HTB is very large of about an order of magnitude difference from a short time of ~100 hours to long times exceeding 100,000 hours at 873 K to 973 K (600 °C to 700 °C). The heat-to-heat variation in time to rupture is mainly explained by the effect of impurities: Al and Ti for the 304HTB and 316HTB, which reduces the concentration of dissolved nitrogen available for the creep strength by the formation of AlN and TiN during creep, and boron for the 347HTB, which enhances fine distributions of $M_{23}C_6$ carbides along grain boundaries. The heat-to-heat variation in time to rupture of the 321HTB is caused by the heat-to-heat variation in grain size, which is inversely proportional to the concentration of Ti. The fundamental creep rupture strength not influenced by impurities is estimated for the steels. The 100,000 hours-fundamental creep rupture strength of the 347HTB steel is lower than that of 304HTB and 316HTB at 873 K and 923 K (600 °C and 650 °C) because the slope of stress *vs* time to rupture curves is steeper in the 347HTB than in the 304HTB and 316HTB. The 100,000 hours-fundamental creep rupture strength of the 321HTB exhibits large variation depending on grain size.

DOI: 10.1007/s11661-016-3587-3


## I. INTRODUCTION

NATIONAL Institute for Materials Science (NIMS) has been conducting the Creep Data Sheet Project since 1966 primarily to obtain the 100,000 hours-creep rupture strength data for principal heat-resistant steels and alloys, which were produced in Japan.[1] The allowable stress for designing high-temperature components is usually determined on the basis of 100,000 hours-creep rupture strength at operating temperature.[2] The establishment of reliable methods for determining the remaining creep life has also been desired for components being operated for a long time because there is an economic advantage in using components beyond the design life. The NIMS Creep Data Sheets have provided long-term creep and creep rupture data available for both safe designing and reliable creep life assessment of high-temperature components.

In the NIMS Creep Data Sheet Project, long-term creep and creep rupture tests have been carried out using multiple heats in each material, *e.g.*, 12 heats for 2.25Cr-1Mo ferritic-pearlitic steel,[3] 10 heats for 9Cr-1Mo-VNb tempered martensitic steel specified as ASME Grade 91,[4] and 9 heats for 18Cr-8Ni austenitic stainless steel,[5] to obtain typical and average test data. The heat means different ingots and different products. The materials such as tubes, pipes, plates, and so on, from which the creep test specimens were taken, were sampled at random from commercial stocks produced in Japan.

It should be noted that the creep test results sometimes exhibit large scattering as shown by about a one order of magnitude difference in creep life or more between the strongest and weakest heats because the creep strength widely depends on production procedures and quality of materials, *e.g.*, heat treatment conditions and impurity contents, and the creep strength is sometimes much lower than that just as one intends, even if

FUJIO ABE, Research Fellow, is with the Materials Reliability Unit, Environment and Energy Materials Division, National Institute for Materials Science (NIMS), 1-2-1 Sengen, Tsukuba 305-0047, Japan. Contact e-mail: ABE.Fujio@nims.go.jp
Manuscript submitted January 25, 2016.
Article published online June 15, 2016

**Table I. Chemical Compositions of 18Cr-8Ni (JIS SUS 304HTB), 18Cr-12Ni-Mo (JIS SUS 316HTB), 18Cr-10Ni-Ti (JIS SUS 321HTB), and 18Cr-12Ni-Nb (JIS SUS 347HTB) Steels Examined**

18Cr-8Ni (JIS SUS 304HTB) (mass pct)

| Heat | C | Si | Mn | P | S | Ni | Cr | Mo | Cu | Ti | Al | | B | N | Nb + Ta | $N_{av}$ (at. pct) | Heat Treatment | Grain Size |
|---|---|---|---|---|---|---|---|---|---|---|---|---|---|---|---|---|---|---|
| | | | | | | | | | | | Sol Al | Insol Al | | | | | | |
| Requirement | 0.04–0.1 | ≤0.75 | ≤2.00 | ≤0.040 | ≤0.030 | 8.00–11.00 | 18.00–20.00 | | | | | | | | | | Rapid cool from 1313 K (1040 °C) or above | |
| ABA | 0.062 | 0.62 | 1.56 | 0.025 | 0.013 | 10.69 | 18.70 | 0.47 | 0.17 | 0.040 | 0.040 | 0.007 | 0.0007 | 0.031 | 0.01 | -0.006 | 1403 K(1130 °C) WQ | 46 |
| ABB | 0.054 | 0.41 | 1.52 | 0.031 | 0.020 | 10.15 | 18.34 | 0.36 | 0.19 | 0.064 | 0.005 | 0.005 | 0.0010 | 0.029 | <0.01 | 0.031 | 1403 K (1130 °C) WQ | 56 |
| ABC | 0.056 | 0.40 | 1.52 | 0.030 | 0.016 | 10.10 | 18.50 | 0.36 | 0.16 | 0.054 | 0.006 | 0.006 | 0.0011 | 0.030 | <0.01 | 0.044 | 1403 K (1130 °C) WQ | 60 |
| ABD | 0.070 | 0.52 | 1.49 | 0.023 | 0.006 | 9.68 | 18.70 | 0.06 | 0.06 | 0.006 | 0.004 | 0.006 | 0.0013 | 0.0270 | <0.01 | 0.092 | (1) | 69 |
| ABE | 0.07 | 0.55 | 1.46 | 0.023 | 0.006 | 9.57 | 18.95 | 0.04 | 0.07 | 0.062 | 0.008 | 0.006 | 0.0018 | 0.0278 | <0.01 | 0.022 | (1) | 60 |
| ABF | 0.08 | 0.62 | 1.34 | 0.021 | 0.006 | 9.80 | 18.25 | 0.06 | 0.05 | 0.020 | 0.008 | 0.005 | 0.0017 | 0.0348 | <0.01 | 0.098 | (1) | 41 |
| ABL | 0.07 | 0.58 | 1.47 | 0.022 | 0.013 | 9.80 | 18.16 | 0.05 | 0.14 | 0.031 | 0.008 | 0.007 | 0.0003 | 0.031 | 0.04 | 0.070 | 1443 K (1170 °C)/10 min WQ | 65 |
| ABM | 0.09 | 0.61 | 1.56 | 0.022 | 0.014 | 10.27 | 18.24 | 0.32 | 0.16 | 0.036 | 0.008 | 0.006 | 0.0001 | 0.038 | 0.03 | 0.092 | 1443 K (1170 °C)/10 min WQ | 63 |
| ABN | 0.07 | 0.60 | 1.58 | 0.022 | 0.012 | 10.26 | 18.18 | 0.31 | 0.12 | 0.040 | 0.008 | 0.006 | 0.0008 | 0.028 | 0.04 | 0.043 | 1443 K (1170 °C)/10 min WQ | 67 |

18Cr-12Ni-Mo (JIS SUS 316HTB) (mass pct)

| Heat | C | Si | Mn | P | S | Ni | Cr | Mo | Cu | Ti | Al | | B | N | Nb + Ta | $N_{av}$ (at. pct) | Heat Treatment | Grain Size |
|---|---|---|---|---|---|---|---|---|---|---|---|---|---|---|---|---|---|---|
| | | | | | | | | | | | Sol Al | Insol Al | | | | | | |
| Requirement | 0.04–0.1 | ≤0.75 | ≤2.00 | ≤0.040 | ≤0.030 | 11.00–14.00 | 16.00–18.00 | 2.00–3.00 | | | | | | | | | | |
| AAA | 0.06 | 0.59 | 1.69 | 0.024 | 0.017 | 13.32 | 16.73 | 2.38 | 0.07 | 0.011 | 0.012 | 0.003 | 0.0010 | 0.030 | 0.02 | 0.0815 | 1383 K (1110 °C)/10 min WQ | 46 |
| AAB | 0.05 | 0.52 | 1.51 | 0.021 | 0.010 | 13.21 | 16.42 | 2.34 | 0.14 | 0.011 | 0.013 | 0.005 | 0.0005 | 0.034 | 0.01 | 0.0954 | 1383 K (1110 °C)/10 min WQ | 56 |
| AAC | 0.05 | 0.71 | 1.52 | 0.022 | 0.013 | 13.50 | 17.50 | 2.28 | 0.17 | 0.055 | 0.023 | 0.004 | 0.0013 | 0.035 | 0.02 | 0.0276 | 1383 K (1110 °C)/10 min WQ | 60 |
| AAD | 0.058 | 0.58 | 1.56 | 0.027 | 0.008 | 13.65 | 16.86 | 2.14 | 0.17 | 0.028 | 0.037 | 0.004 | 0.0009 | 0.025 | 0.01 | -0.0095 | 1403 K (1130 °C) WQ | 69 |
| AAE | 0.078 | 0.62 | 1.60 | 0.021 | 0.008 | 13.51 | 16.90 | 2.08 | 0.16 | 0.037 | 0.027 | 0.004 | 0.0010 | 0.028 | 0.01 | 0.0125 | 1403 K (1130 °C) WQ | 60 |
| AAF | 0.066 | 0.63 | 1.73 | 0.029 | 0.024 | 13.16 | 17.07 | 2.34 | 0.13 | 0.055 | 0.092 | 0.003 | 0.0020 | 0.028 | 0.01 | -0.1417 | 1403 K (1130 °C) WQ | 41 |
| AAL | 0.07 | 0.61 | 1.65 | 0.025 | 0.007 | 13.60 | 16.60 | 2.33 | 0.26 | 0.043 | 0.009 | 0.008 | 0.0011 | 0.0250 | 0.01 | 0.0307 | (1) | 65 |
| AAM | 0.06 | 0.52 | 1.60 | 0.025 | 0.007 | 13.30 | 16.70 | 2.25 | 0.24 | 0.060 | 0.012 | 0.008 | 0.0008 | 0.0318 | 0.01 | 0.0318 | (1) | 63 |
| AAN | 0.06 | 0.52 | 1.58 | 0.025 | 0.007 | 13.60 | 16.60 | 2.31 | 0.26 | 0.029 | 0.011 | 0.010 | 0.0007 | 0.0224 | 0.01 | 0.0326 | (1) | 67 |

18Cr-10Ni-Ti (JIS SUS 321HTB) (mass pct)

| Heat | C | Si | Mn | P | S | Ni | Cr | Mo | Cu | Ti | Al | B | N | Nb + Ta | Heat Treatment | Grain Size |
|---|---|---|---|---|---|---|---|---|---|---|---|---|---|---|---|---|
| Requirement | 0.04–0.1 | ≤0.75 | ≤2.00 | ≤0.040 | ≤0.030 | 9.00–13.00 | 17.00–20.00 | | | 4 × C pct − 0.60 | | | | | (2) | |
| ACA | 0.07 | 0.62 | 1.49 | 0.023 | 0.006 | 11.23 | 17.80 | 0.11 | 0.09 | 0.39 | 0.013 | 0.0001 | 0.0116 | <0.01 | (1) | 92 |
| ACB | 0.07 | 0.54 | 1.59 | 0.023 | 0.006 | 10.92 | 18.20 | 0.10 | 0.09 | 0.47 | 0.058 | 0.0006 | 0.0092 | 0.02 | (1) | 83 |
| ACC | 0.06 | 0.57 | 1.46 | 0.023 | 0.006 | 10.92 | 17.90 | 0.08 | 0.11 | 0.42 | 0.023 | 0.0010 | 0.0106 | 0.02 | (1) | 65 |
| ACG | 0.080 | 0.53 | 1.60 | 0.023 | 0.007 | 12.61 | 18.61 | 0.09 | 0.08 | 0.51 | 0.065 | 0.0001 | 0.0083 | <0.01 | 1453 K (1180 °C) WQ | 31 |
| ACH | 0.068 | 0.47 | 1.59 | 0.023 | 0.015 | 12.46 | 18.82 | 0.09 | 0.08 | 0.52 | 0.020 | 0.0007 | 0.0074 | <0.01 | 1453 K (1180 °C) WQ | 31 |
| ACJ | 0.078 | 0.55 | 1.65 | 0.023 | 0.006 | 12.55 | 18.70 | 0.16 | 0.06 | 0.55 | 0.029 | 0.0003 | 0.008 | <0.01 | 1453 K (1180 °C) WQ | 31 |

**Table I. continued**

18Cr-10Ni-Ti (JIS SUS 321HTB) (mass pct)

| Heat | C | Si | Mn | P | S | Ni | Cr | Mo | Cu | Ti | Al | B | N | Nb + Ta | Heat Treatment | Grain Size |
|---|---|---|---|---|---|---|---|---|---|---|---|---|---|---|---|---|
| ACL | 0.06 | 0.55 | 1.56 | 0.026 | 0.010 | 12.27 | 18.02 | 0.02 | 0.06 | 0.49 | 0.121 | 0.0005 | 0.014 | <0.01 | 1393 K (1120 °C)/10min WQ | 63 |
| ACM | 0.06 | 0.54 | 1.67 | 0.028 | 0.016 | 12.62 | 17.71 | 0.02 | 0.05 | 0.53 | 0.161 | 0.0002 | 0.013 | <0.01 | 1393 K (1120 °C)/10min WQ | 47 |
| ACN | 0.06 | 0.61 | 1.74 | 0.020 | 0.006 | 12.59 | 17.86 | 0.25 | 0.06 | 0.39 | 0.040 | 0.0010 | 0.019 | <0.01 | 1393 K (1120 °C)/10min WQ | 69 |

18Cr-12Ni-Nb (JIS SUS 347HTB) (mass pct)

| Heat | C | Si | Mn | P | S | Ni | Cr | Mo | Cu | Ti | Al | B | N | Nb + Ta | Nb/C (atomic ratio) | Heat Treatment | Grain Size |
|---|---|---|---|---|---|---|---|---|---|---|---|---|---|---|---|---|---|
| Requirement | 0.04–0.1 | ≤0.75 | ≤2.00 | ≤0.040 | ≤0.030 | 9.00–13.00 | 17.00–20.00 | | | | | | | 8 × C pct − 1.0 | | (2) | |
| AEA | 0.07 | 0.60 | 1.71 | 0.020 | 0.005 | 12.00 | 17.85 | 0.04 | 0.05 | 0.019 | 0.019 | 0.0012 | 0.0284 | 0.74 | 1.37 | (1) | 54 |
| AEB | 0.06 | 0.49 | 1.66 | 0.023 | 0.006 | 12.20 | 17.80 | 0.05 | 0.03 | 0.018 | 0.023 | 0.0012 | 0.0236 | 0.82 | 1.77 | (1) | 69 |
| AEC | 0.07 | 0.62 | 1.73 | 0.024 | 0.007 | 12.20 | 17.95 | 0.10 | 0.04 | 0.019 | 0.012 | 0.0016 | 0.0216 | 0.72 | 1.33 | (1) | 56 |
| AED | 0.04 | 0.82 | 1.73 | 0.022 | 0.009 | 12.50 | 17.61 | 0.06 | 0.10 | 0.019 | 0.013 | 0.0004 | 0.020 | 0.79 | 2.55 | 1473 K (1200 °C)/20 min WQ | 77 |
| AEE | 0.05 | 0.80 | 1.70 | 0.019 | 0.011 | 12.21 | 17.26 | 0.07 | 0.09 | 0.018 | 0.012 | 0.0003 | 0.021 | 0.77 | 1.99 | 1473 K (1200 °C)/20 min WQ | 88 |
| AEF | 0.05 | 0.77 | 1.74 | 0.025 | 0.007 | 12.55 | 17.89 | 0.11 | 0.09 | 0.020 | 0.004 | 0.0004 | 0.016 | 0.77 | 1.99 | 1473 K (1200 °C)/20 min WQ | 121 |
| AEG | 0.053 | 0.63 | 1.81 | 0.027 | 0.011 | 12.24 | 17.56 | 0.15 | 0.14 | 0.019 | 0.008 | 0.0027 | 0.0222 | 0.87 | 2.12 | 1403 K (1130 °C) WQ | 58 |
| AEH | 0.065 | 0.49 | 1.76 | 0.019 | 0.027 | 12.13 | 18.05 | 0.06 | 0.08 | 0.036 | 0.007 | 0.0018 | 0.0241 | 0.88 | 1.75 | 1403 K (1130 °C) WQ | 67 |
| AEJ | 0.060 | 0.54 | 1.82 | 0.028 | 0.012 | 12.38 | 17.70 | 0.19 | 0.11 | 0.019 | 0.007 | 0.0020 | 0.0223 | 0.87 | 1.87 | 1403 K (1130 °C) WQ | 58 |

(1) Solution temperature was not described in mill sheets.
(2) Rapid cool from 1368 K (1095 °C) or above and from 1323 K (1050 °C) or above for cold worked and hot rolled tubes, respectively.

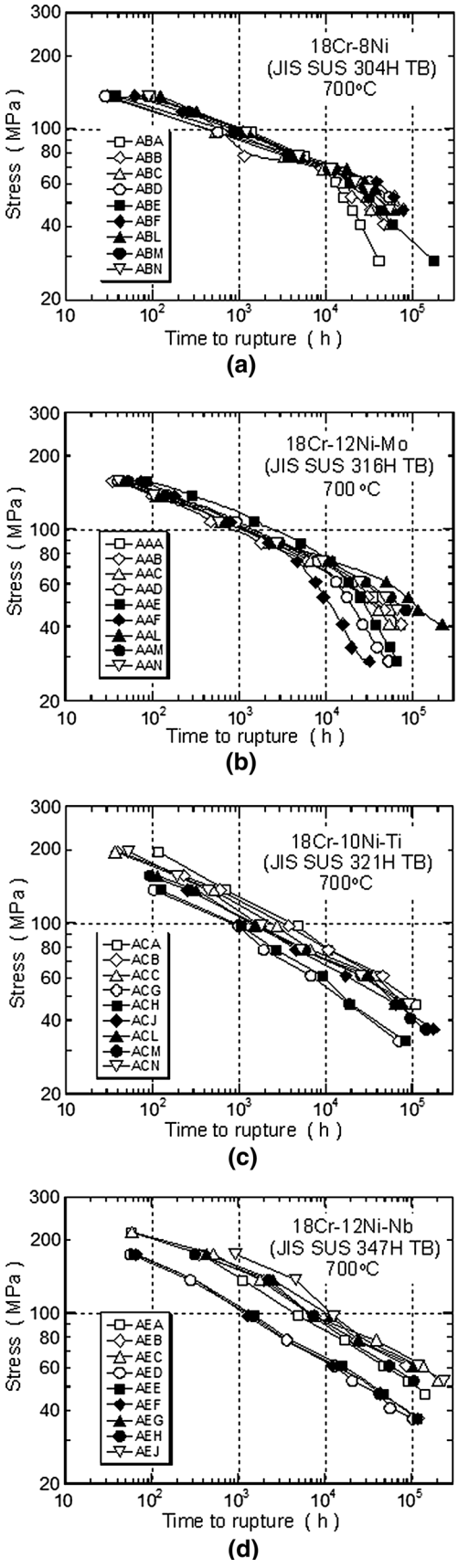


Fig. 1—Creep rupture data for respective heats of (*a*) 304HTB, (*b*) 316HTB, (*c*) 321HTB, and (*d*) 347HTB at 973 K (700 °C).

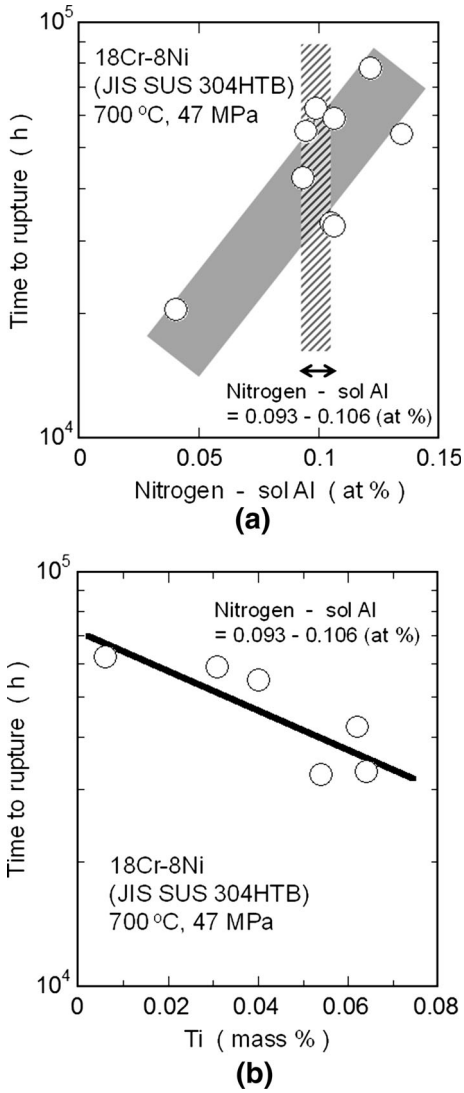


Fig. 2—(*a*) Time to rupture of 304HTB at 973 K (700 °C) and 47 MPa, as a function of (N – sol Al) concentration and (*b*) Ti concentration dependence of time to rupture at (N – sol Al) concentration of 0.093 to 0.106 at. pct.

the material is well alloy-designed.[6–8] The large scattering of creep rupture data also makes it difficult to assess long-term creep strength satisfactorily. Because the NIMS Creep Data Sheets contain a full set of data, such as not only creep rupture data, minimum creep rates, time to tertiary creep, and short-time tensile data but also the details of material production procedures and chemical compositions, we can analyze the origins of difference in creep life among different heats by using data in the NIMS Creep Data Sheets.

The present author has revealed for some high-Cr martensitic steels that the heat-to-heat variation in long-term creep life is correlated with the degradation behavior at long times, which depends on initial strength and concentrations of impurities Al and Ti and of major alloying element Cr.[8] The large initial strength resulting from low-temperature tempering and, hence, high

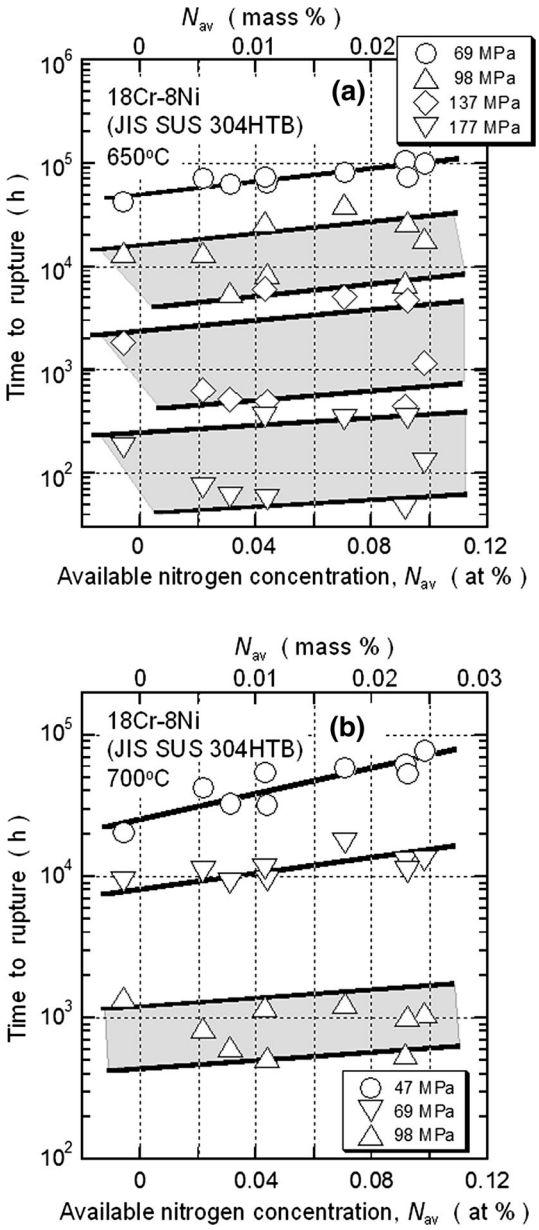


Fig. 3—Time to rupture of 304HTB steel at (*a*) 923 K (650 °C) and (*b*) 973 K (700 °C), as a function of available nitrogen concentration $N_{av}$.

density of dislocations causes the large driving force for microstructure recovery during creep. It has been well known that nitrogen has a beneficial effect on the long-term creep strength of heat-resistant steels. But the concentration of nitrogen available for the creep strength is reduced by the formation of AlN and TiN during creep because Al and Ti are strong nitride-forming elements. The reduction of nitrogen concentration results in the degradation in creep strength in plain 12Cr and 12Cr-1Mo-1W-0.3V steels for turbine at long times. The higher concentrations of Al and Ti accelerate the degradation in creep strength at long times. The degradation in creep strength at long times by the formation of AlN has also been investigated for a variety of heat-resistant steels, such as martensitic 9Cr

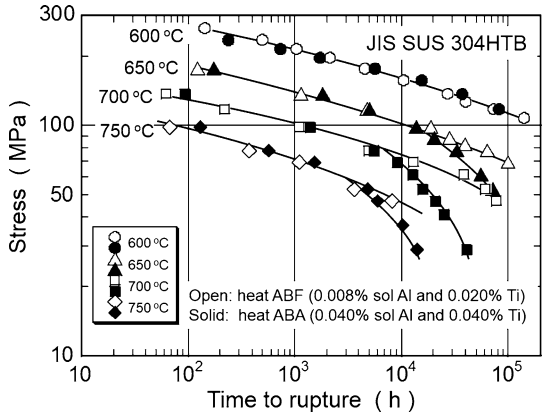


Fig. 4—Creep rupture data for heat ABF with low sol Al and low Ti and for heat ABA with high sol Al and high Ti of 304HTB at 873 K to 1023 K (600 °C to 750 °C).

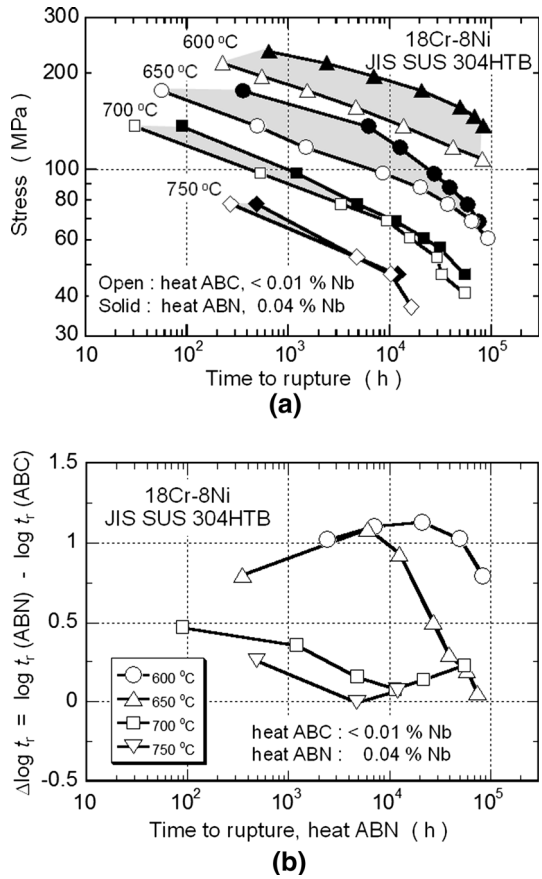


Fig. 5—(*a*) Creep rupture data for heat ABC (lower than 0.01 pct Nb) and heat ABN (0.04 pct Nb) of 304HTB and (*b*) difference in logarithm of time to rupture between the two heats *vs* time to rupture of heat ABN.

steels of ASME Grade 91 (9Cr-1Mo-VNb)[9,10] and ASME Grade 92 (9Cr-0.5Mo-1.8W-VNb)[11] and austenitic type 304[12] and type 316[13] stainless steels. The high concentration of Cr above 11 pct also accelerates the degradation in creep strength of the 12Cr-1Mo-1W-0.3V steel at long times.[8]

The purpose of the present research is to investigate metallurgical factors causing the heat-to-heat variation in creep life for 300 series stainless steels for boiler and heat exchanger seamless tubes, 18Cr-8Ni (JIS SUS 304HTB), 18Cr-12Ni-Mo (JIS SUS 316HTB), 18Cr-10Ni-Ti (JIS SUS321 HTB), and 18Cr-12Ni-Nb (JIS SUS 347HTB), using data in the NIMS Creep Data Sheets. The JIS, SUS, and HTB stand for the Japanese Industrial Standard, Steel Use Stainless, and hot worked stainless steel boiler and heat exchanger tubes, respectively. In the following, these steels are denoted as 304HTB, 316HTB, 321HTB, and 347HTB, respectively. The 300 series stainless steels are widely used in high-temperature components because austenitic stainless steels are superior to 2.25 to 3Cr bainitic steels and 9 to 12Cr martensitic steels in terms of having higher creep strength due to lower self-diffusion rates arising from a close-packed, face-centered cubic crystal structure as well as good oxidation resistance due to higher Cr and Ni concentrations. The fundamental creep rupture strength, which is defined as the creep rupture strength not influenced by impurities, is also estimated by eliminating the impurity effects from the test results on creep life of the steels. Based on the fundamental creep rupture strength, we can understand the creep strength of commercial stocks of these steels, which contain a variety of impurities in different amounts, by taking the impurity effect into account.

## II. MATERIALS AND CREEP RUPTURE TESTING

The present author analyzed the creep rupture data for the individual heats of the 304HTB,[5] 316HTB,[14] 321HTB,[15] and 347HTB[16] in the NIMS Creep Data Sheets. The NIMS Creep Data Sheets contain the creep rupture data for nine heats of the respective steels. The chemical compositions of individual heats of the steels

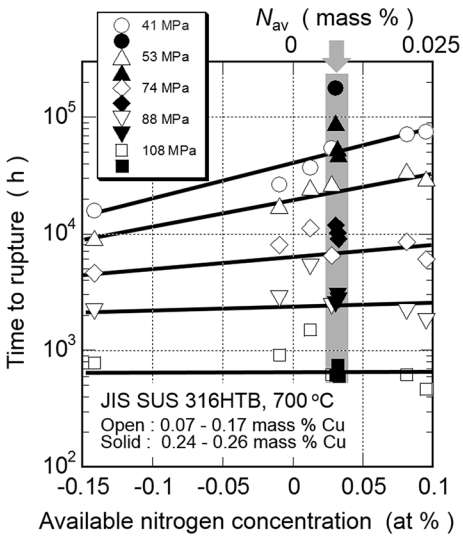


Fig. 6—Time to rupture of 316HTB at 973 K (700 °C), as a function of available nitrogen concentration $N_{av}$.

are given in Table I, which basically transcribes the mill sheets submitted by respective tube suppliers, together with the requirements of chemical compositions by JIS. The name of heat such as ABA is due to the reference code in the NIMS Creep Data Sheets. The tubes were sampled at random from commercial stocks produced in Japan in the late 1960s. The chemical analysis of the steels was carried out by induction coupled plasma (ICP) emission spectroscopy[17] because of its high-speed analysis for number of elements. In the ICP, the light emitted by the atoms of an element in solution is used for analysis because each element has many specific wavelengths in the spectrum. Unfortunately, the spectra from Nb and Ta could not be distinguished from each other because the accuracy for spectra analysis was not so high in the 1960s. Therefore, the name of elements relating to Nb is shown as Nb + Ta in Table I. But it is practically Nb, as shown by a Nb peak by energy-dispersive characteristic X-ray analysis for precipitate particles, which will be shown in a later section. The concentration of Nb is not specified for 304HTB by JIS, and it is rather low in the present 304HTB. The heats ABL, ABM, and ABN of the 304HTB contain 0.03 to 0.04 pct Nb, whereas the concentration of Nb in the other heats is substantially zero. The sol and insol Al in Table I mean soluble Al and insoluble Al of $Al_2O_3$, respectively. In this article, soluble Al is used as the concentration of Al for the analysis of creep strength because soluble Al forms AlN during creep. In the 304HTB and 316HTB, the impurity Al mainly consists of soluble Al, which is given by (sol Al) = (total Al) − 0.006 (mass pct).

The creep rupture test specimens, having a size of 6 mm gauge diameter and 30 mm gauge length, were taken longitudinally from the as-received tubes with 50 mm outer diameter and 8 mm wall thickness. The tubes had already been solution-annealed. Creep rupture testing was carried out at 873 K to 1123 K (600 °C to 850 °C), 873 K to 1023 K (600 °C to 750 °C), 823 K to 1048 K (550 °C to 775 °C), and 873 K to 1023 K (600 °C to 750 °C) for the 304HTB, 316HTB, 321HTB, and 347HTB, respectively. The maximum time to rupture was 222,705.3 hours. The details of the creep rupture test procedure are described in the NIMS Creep Data Sheets.

## III. HEAT-TO-HEAT VARIATION IN CREEP LIFE

### A. *Creep Rupture Data*

Figure 1 shows the creep rupture data for the 304HTB, 316HTB, 321HTB, and 347HTB at 973 K (700 °C). For the four steels, each heat exhibits its distinct stress dependence of time to rupture. This indicates that the heat-to-heat variation in time to rupture is not caused by data scattering at random but instead involves specific mechanisms. The heat-to-heat variation in time to rupture of the 304HTB and 316HTB is quite different from that of the 321HTB and 347HTB. The heat-to-heat variation in time to rupture of the 304HTB and 316HTB is not large at short times less than 1000 hours, but it becomes more significant when

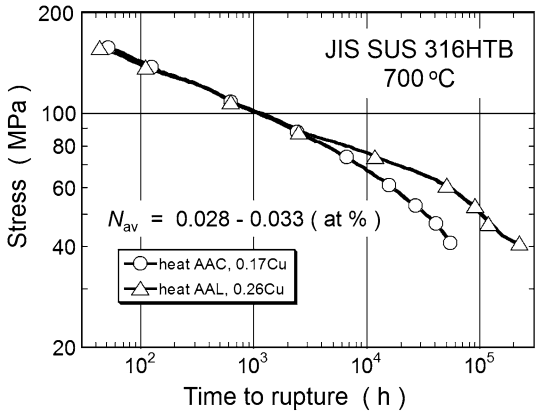


Fig. 7—Comparison of creep rupture data between low and high Cu heats of 316HTB at 973 K (700 °C).

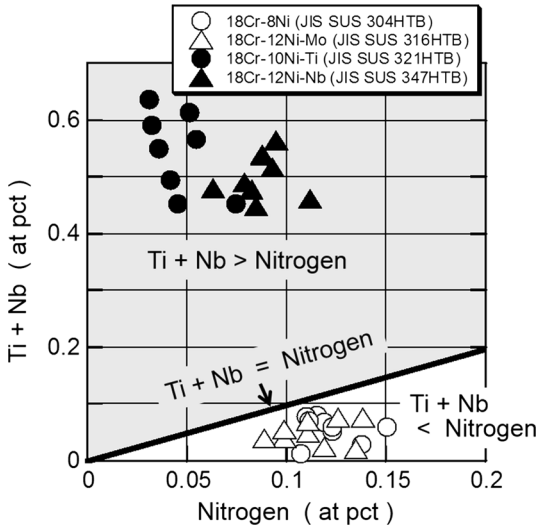


Fig. 8—Concentration of Ti plus Nb *vs* that of nitrogen in atomic pct in respective heats of the steels.

the test duration is increased at long times above about 10,000 hours. The onset time for increasing the heat-to-heat variation in time to rupture shifts to longer times at lower temperatures of 873 K and 923 K (600 °C and 650 °C) than at a high temperature of 973 K (700 °C), indicating diffusion-controlled microstructure evolution is involved in the heat-to-heat variation in time to rupture. On the other hand, the heat-to-heat variation in time to rupture of the 321HTB and 347HTB is very large as shown by about one order of magnitude difference between the strongest and weakest heats even at a short time of about 100 hours. Substantially the same magnitude of heat-to-heat variation in time to rupture continues for up to long times exceeding 100,000 hours. This is also typical at low temperatures of 873 K and 923 K (600 °C and 650 °C).

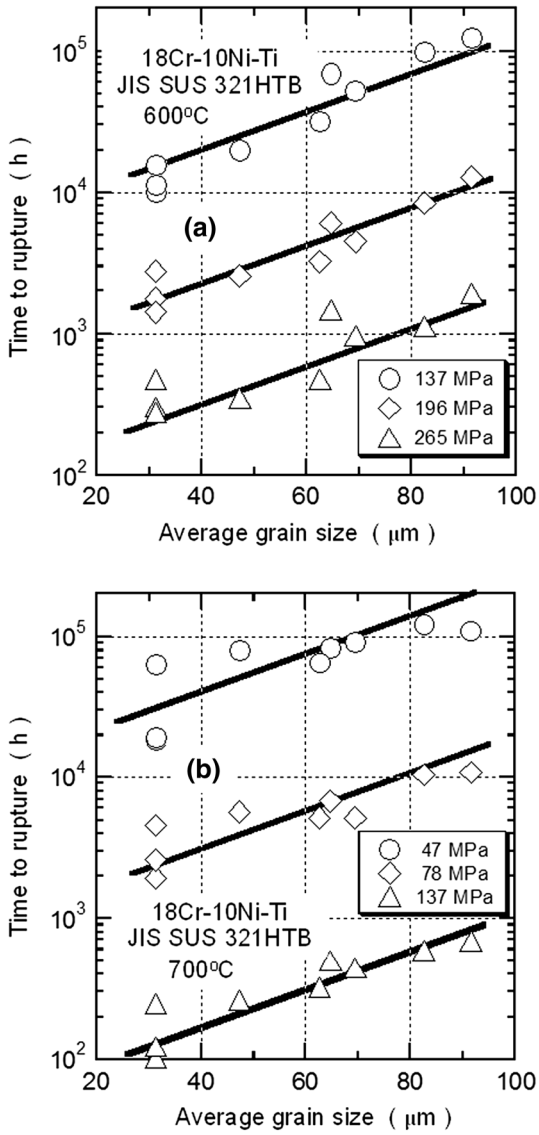


Fig. 9—Time to rupture of 321HTB at (*a*) 873 K (600 °C) and (*b*) 973 K (700 °C), as a function of average grain size.

## B. *Effect of Impurities on Heat-to-Heat Variation in Creep Life of 304HTB and 316HTB*

There is no distinct relationship between the time to rupture and grain size and between the time to rupture and initial strength of 0.2 pct offset proof stress and ultimate tensile strength at the creep test temperature for the different heats of 304HTB and 316HTB. Therefore, these parameters are excluded as the explanation of the observed heat-to-heat variation in time to rupture of the 304HTB and 316HTB.

It has been well known that nitrogen has a beneficial effect on long-term creep strength of heat-resistant steels through its solid solution hardening as well as

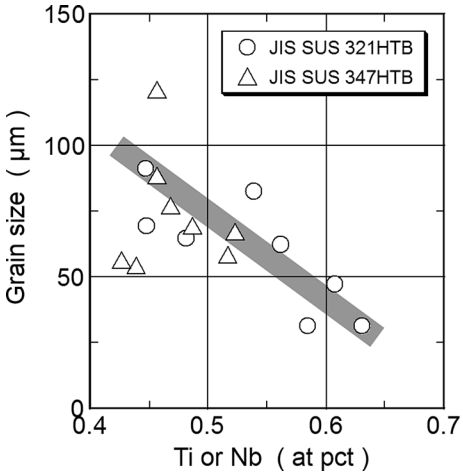


Fig. 10—Ti and Nb concentrations *vs* grain size for 321HTB and 347HTB.

precipitate hardening by forming fine nitrides. But the concentration of nitrogen available for the creep strength is reduced by the formation of AlN during creep because Al is a strong nitride-forming element. The concentrations of Al and nitrogen, which are not specified by JIS, are rather low in the present 304HTB and 316HTB, but they are substantially different among the different heats (Table I). Figure 2(a) shows the time to rupture of 304HTB at 973 K (700 °C) and 47 MPa, as a function of (N–sol Al) concentration, where N means the concentration of nitrogen. Although the time to rupture has a tendency to increase with increasing (N–sol Al) concentration, the variation of time to rupture is still large even at the same (N–sol Al) concentration. At the same (N–sol Al) concentration of 0.093 to 0.106 at. pct as shown by the hatched zone in Figure 2(a), the time to rupture varies from 32,453 to 62,414 hours. This is due to the effect of Ti as shown in Figure 2(b). Ti is also a strong nitride-forming element, similar to Al. The variation of atomic concentration of Ti among the nine heats of the present 304HTB (0.007 to 0.074 at. pct Ti, corresponding to 0.006 to 0.064 mass pct Ti) is approximately the same as that of sol Al (0.008 to 0.082 at. pct sol Al, corresponding to 0.004 to 0.040 mass pct sol Al). Therefore, the variation of Ti concentration cannot be ignored in the analysis of heat-to-heat variation in time to rupture. On the other hand, the variation of nitrogen concentration among the different heats is very small as given by the narrow range of $0.030 \pm 0.005$ mass pct for the most heats of 304HTB and 316HTB.

Figure 3 shows the time to rupture of the nine heats of 304HTB at 923 K and 973 K (650 °C and 700 °C) as a function of available nitrogen concentration. The available nitrogen concentration is defined as the concentration of nitrogen free from AlN and TiN.[6] Nitrogen free from AlN and TiN, such as dissolved nitrogen and fine nitrides, is considered to be available for strengthening in creep of heat-resistant steels, and hence, the creep life is proportional to the available nitrogen concentration. The formation of AlN rods was observed in the present 304HTB[12] and 316HTB[13] after long-term creep. Assuming the formation of stoichiometric compounds of AlN and TiN, the available nitrogen concentration $N_{av}$ is described as:

$$N_{av} = \text{N} - \text{sol Al} - \text{Ti(at. pct)} \quad [1]$$

where N, sol Al, and Ti are the concentration of nitrogen, soluble Al, and Ti, respectively, in at. pct.[8] The available nitrogen concentration in at. pct is given in Table I. The available nitrogen concentration is also expressed in mass pct as:

$$\begin{aligned} N_{av} &= \text{N} - 0.519\text{sol Al} - 0.292\text{Ti(mass pct)} \\ &= 1/4 N_{av}\text{(at. pct)} \end{aligned} \quad [2]$$

Zr is also a strong nitride-forming element, similar to Al and Ti. Usually, the concentration of Zr is very low in heat-resistant steels and hence the effect of Zr can be neglected.

In Figure 3, the logarithm of time to rupture simply increases with increasing available nitrogen concentration and the slope of logarithm of time to rupture *vs* available nitrogen concentration curve ($\Delta\log t_r/\Delta N_{av}$) increases with decreasing stress and with increasing test duration. The slope ($\Delta\log t_r/\Delta N_{av}$) is evaluated to be 12.6, 16.8, 18.2, and 20.6/at. pct $N_{av}$ at 177, 137, 98, and 69 MPa, respectively, at 923 K (650 °C) and 11.5, 18.5 and 31.6/at. pct $N_{av}$ at 98, 69, and 47 MPa, respectively, at 973 K (700 °C). The effect of nitrogen on creep at long times is considered to be mainly due to solid solution hardening by the interaction between dislocations and dissolved nitrogen atoms rather than to precipitation hardening by nitrides because nitrides can coarsen during long-term creep, resulting in being unavailable for hardening at long times. The same behavior has also been reported for the 12Cr martensitic steel specified as JIS SUS 403-B and for the 12Cr-1Mo-1W-0.3V martensitic steel specified as JIS SUH 616.[8] The present results in Figure 3 suggest that the increase in time to rupture by a decrease in stress is less significant in the heats with higher Al and Ti, namely, with lower $N_{av}$. The amount of AlN and TiN formed during creep increases with increasing test duration, which is more significant in the heats with higher Al and Ti, namely, with lower $N_{av}$. After completion of the formation of AlN and TiN during creep, we can expect no change in slope of the curve any more. The increase in slope of the curve with time for up to about 100,000 hours at 973 K (700 °C) shown in Figure 3 suggests that the formation of AlN and TiN is still continuing even at long times of about 100,000 hours at 973 K (700 °C) but not completed as yet, although the kinetics of nitride precipitation is not clear because of no measurement of the amount of nitrides. The available nitrogen concentration $N_{av}$ of the heat ABA exhibits a minus value as given in Table I because of a high concentration of sol Al and Ti. Although the minimum value of concentration is zero but not a minus value, the available nitrogen concentration represents the magnitude of driving force for the formation of AlN and TiN during creep.

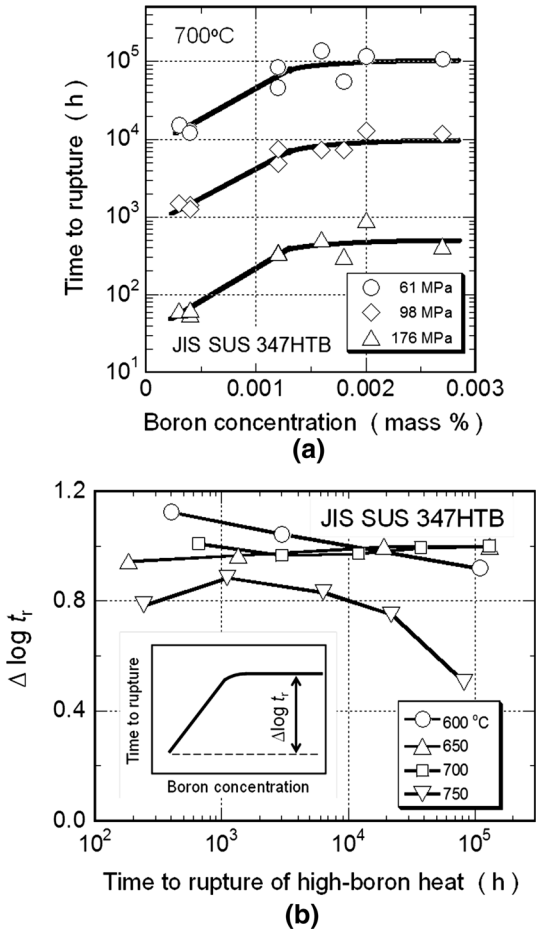


Fig. 11—(*a*) Time to rupture *vs* boron concentration and (*b*) difference in logarithm of time to rupture between high-boron and low-boron heats of 347HTB, as a function of time to rupture of high-boron heat. The high- and low-boron heats contain 15 to 27 and 3 to 4 ppm boron, respectively.

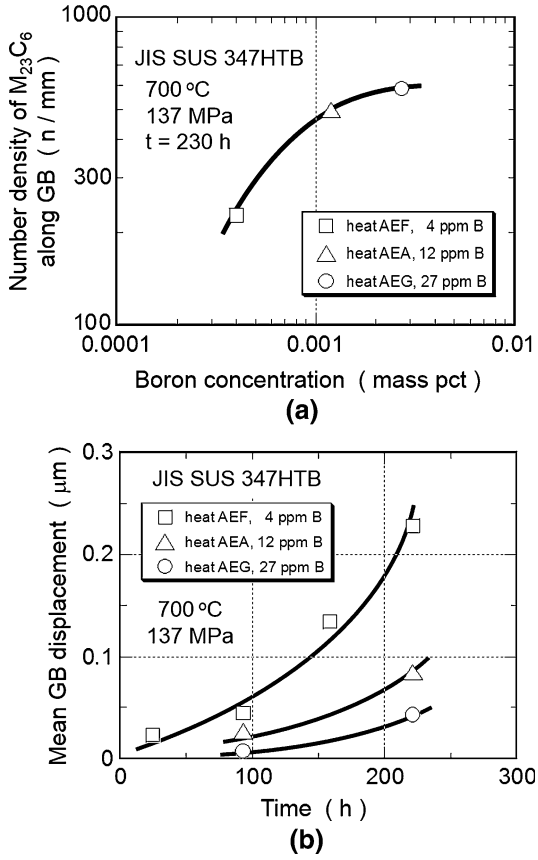


Fig. 12—(*a*) Relationship between number density of $M_{23}C_6$ carbides along grain boundary and boron concentration after interrupting creep test at 230 h, and (*b*) mean grain boundary displacement for the heats of 347HTB during creep at 973 K (700 °C) and 137 MPa.

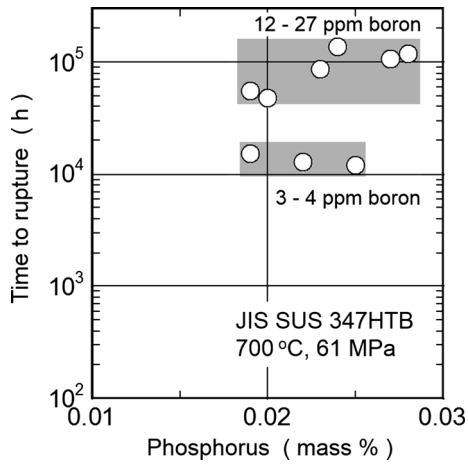


Fig. 13—Relationship between time to rupture and phosphorus concentration of nine heats of 347HTB at 973 K (700 °C) and 61 MPa.

Figure 4 shows the creep rupture data for the heat ABA, containing high sol Al of 0.040 and high Ti of 0.040 mass pct, at 873 K to 1023 K (600 °C to 750 °C), compared with those for the heat ABF, containing low sol Al of 0.008 and low Ti of 0.020 mass pct. The degradation in creep rupture strength of the heat ABA takes place at earlier times with increasing test temperature, indicating diffusion-controlled formation of AlN and TiN during creep. The degradation in creep rupture strength can take place even at 873 K (600 °C), but it needs longer times above about 100,000 hours, which was the longest test duration at 873 K (600 °C) because of lower temperature.

Traditionally the nitrogen-to-aluminum ratio (N/Al), where the concentrations of N and Al are in mass pct, has been used for the analysis of effect of nitrogen and aluminum on the creep strength of heat-resistant steels.[9,10] However, the time to rupture depends on the concentration of Ti as well as on those of nitrogen and sol Al, as already shown in Figures 2 and 3. The present results indicate that the available nitrogen concentration $N_{av}$ described by Eqs. [1] and [2] gives us reliable analysis of the heat-to-heat variation in time to rupture of 304HTB.

In Figure 3, the available nitrogen concentration dependence of time to rupture is split into the two lines at high stress and short time conditions. The line with a longer time to rupture represents the data for the heats

ABA, ABL, ABM, and ABN containing 0.01 to 0.04 pct Nb, whereas that with shorter time to rupture is for the heats ABB, ABC, ABD, ABE, and ABF containing less than 0.01 pct Nb, substantially no Nb. Figure 5(a) shows the creep rupture data for the heats ABC and ABN of 304HTB containing substantially no Nb and 0.04 pct Nb, respectively, at 873 K to 1023 K (600 °C to 750 °C). The available nitrogen concentration of the two heats is substantially the same, $N_{av}$ = 0.043 to 0.044 (at. pct). The difference in logarithm of time to rupture $\Delta(\log t_r)$ between the two heats at the same stress conditions is shown in Figure 5(b) as a function of time to rupture of the heat ABN. The $\Delta(\log t_r)$ increases at first and then decreases at long times after reaching a peak. With decreasing temperature, the time to reach a peak shifts to longer times, whereas the peak height increases. This is typical in age-hardening behavior in alloys. The $\Delta\log t_r$ curves exhibit a small increase at long times at 973 K and 1023 K (700 °C and 750 °C). The mechanisms for the small increase at long times are at present not clear.

The TEM observations of the heats ABC and ABN after creep rupture testing at 923 K (650 °C) and 137 MPa, at which the time to rupture was 496.8 and 6064.8 hours for the heats ABC and ABN, respectively, showed that not only the $M_{23}C_6$ carbides having a size of about 0.2 $\mu$m but also very fine and high-density NbC carbides having a size of about 10 nm had precipitated during creep in the heat ABN.[7] The identification of NbC carbides was carried out by energy-dispersive characteristic X-ray analysis. In the heat ABC, only the $M_{23}C_6$ carbides had homogeneously precipitated in the matrix during creep but no NbC carbide. The dislocation density was much higher in the heat ABN than in the heat ABC, resulting from the pinning by high-density NbC carbides. The present results suggest that the difference in time to rupture between the heats ABC and ABN in Figure 5 is caused by the precipitation hardening due to fine NbC carbides. The coarsening of very fine NbC carbides and the recovery of dislocations took place at long times during creep. The precipitation hardening due to fine NbC carbides significantly increases the creep life of the heat ABN at short times for up to 6000 hours at 923 K (650 °C) (Figure 5), but it becomes less pronounced at long times by the coarsening of fine NbC carbides during creep. The diffusion-controlled precipitation of fine NbC carbides from supersaturated solid solution and subsequent coarsening shift the $\Delta(\log t_r)$ *vs* time curves in Figure 5(b) to longer times with decreasing temperature.

The $\sigma$ phase particles precipitated mainly at grain boundaries in the 304HTB steel at long times above about 2000 hours at 973 K (700 °C), although the density of $\sigma$ phase particles was very low.[12] The contribution of $\sigma$ phase to the creep strength of 304HTB seems to be small because of low density, indicating substantially no influence on the heat-to-heat variation of time to rupture, as will be described in detail in a later section of this article.

The concept of available nitrogen concentration is also applied to the 316HTB as the main explanation of heat-to-heat variation in time to rupture. Figure 6 shows the time to rupture of the nine heats of 316HTB at 973 K (700 °C) as a function of available nitrogen concentration $N_{av}$. The time to rupture simply increases with increasing available nitrogen concentration, which becomes more significant with decreasing stress and increasing test duration. At approximately the same available nitrogen concentration of $N_{av}$ = 0.028 to 0.022 at. pct, shown by the arrow in Figure 6, the time to rupture widely differs at low stresses and long times. This is correlated with the variation of impurity Cu among the different heats. The concentration of Cu varies from 0.07 to 0.26 mass pct in the present 316HTB (Table I). The heats with high Cu (0.24 to 0.26 mass pct) exhibit the longer time to rupture at long times above about 2000 to 3000 hours at 973 K (700 °C), as shown in Figure 7.

In the 316HTB, the precipitation of $M_{23}C_6$ carbides take place in the matrix and at grain boundaries in the initial stage of creep and then the precipitation of $Fe_2Mo$ Laves phase and $\sigma$ phase takes place at long times mainly in the matrix and at grain boundaries, respectively. We observed that the coarsening rate of $M_{23}C_6$ carbides was smaller in the heats with high Cu than in those with low Cu during creep.

It is concluded that the heat-to-heat variation in time to rupture of the 304HTB and 316HTB is mainly caused by the heat-to-heat variation in available nitrogen concentration and that the effect of a small amount of impurities Nb and Cu is overlapped in the 304HTB and 316HTB, respectively.

### C. *Metallurgical Factors Causing Heat-to-Heat Variation in Creep Life of 321HTB and 347HTB*

The concept of available nitrogen concentration cannot be applied to the 321HTB and 347HTB, which are alloyed with the strong nitride-forming elements Ti and Nb, respectively. Figure 8 compares the atomic concentration of Ti plus Nb with that of nitrogen in the 304HTB, 316HTB, 321HTB, and 347HTB. In the 304HTB and 316HTB, the atomic concentration of Ti plus Nb is much lower than that of nitrogen, and hence, most nitrogen atoms are dissolved in solid solution after the solution treatment, even if impurities Ti and Nb form inclusions of nitrides at a high temperature. In the 321HTB and 347HTB, on the other hand, the atomic concentration of Ti plus Nb is much higher than that of nitrogen, because the present 321HTB and 347HTB are alloyed with 0.39 to 0.55 mass pct Ti and 0.72 to 0.88 mass pct Nb, respectively (Table I). We observed a large number of inclusions of Ti- and Nb-carbonitrides in the 321HTB and 347HTB, respectively, in as-received condition. This suggests that the concentration of dissolved nitrogen is very low or substantially zero after solution treatment. Therefore, the scenario that dissolved nitrogen present after solution treatment forms

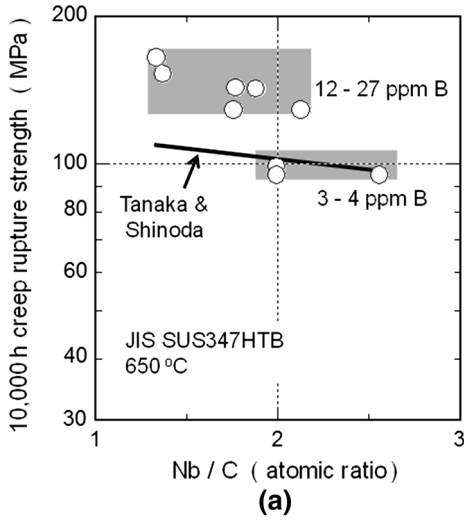


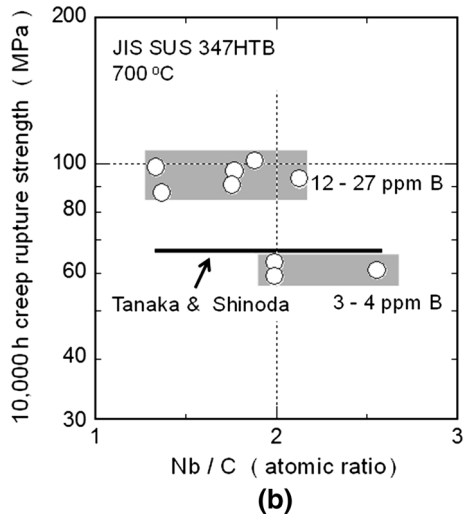


Fig. 14—Relationship between 10,000 hour-creep rupture strength and Nb/C atomic ratio for nine heats of 347HTB at (*a*) 923 K (650 °C) and (*b*) 973 K (700 °C), together with results by Tanaka and Shinoda[31] for 18Cr-10Ni-Nb steel.

AlN and TiN during creep cannot be applied to the 321HTB and 347HTB and, hence, other factors cause the observed heat-to-heat variation in time to rupture.

1. *Effect of grain size on heat-to-heat variation in creep life of 321HTB*

Figure 9 shows the time to rupture of the nine heats of 321HTB at 873 K and 973 K (600 °C and 700 °C) as a function of average grain size. The average grain size is given in Table I. In the NIMS Creep Data Sheets, the method for determining average grain size was due to the comparison procedure, JIS G 0551,[18] which corresponds to ASTME E112.[19] This procedure involves comparison of observed optical micrographs of representative fields of the test specimens at a magnification of 100 times with a series of graded reference images. The logarithm of time to rupture linearly increases with increasing average grain size as:

$$\Delta(\log t_r) / \Delta d = 0.0132/\mu\text{m} \qquad [3]$$

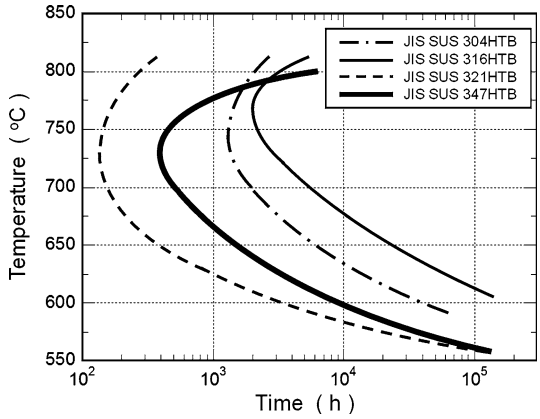


Fig. 15—Time-temperature-precipitation diagram for $\sigma$ phase in 304HTB, 316HTB, 321HTB, and 347HTB.

where $d$ is the average diameter of grains in $\mu$m. The same grain size dependence of the increase in logarithm of time to rupture in Eq. [3], namely, the same proportional constant of 0.0132, is also observed at other test temperatures of 923 K and 1023 K (650 °C and 750 °C). Equation [3] means that if the diameter of grains increases 10 $\mu$m, the time to rupture increases 1.36 times of the original value. The present results indicate that the heat-to-heat variation in time to rupture of 321HTB is caused by the heat-to-heat variation in grain size.

The average grain size of the 321HTB decreases with increasing the concentration of Ti, as shown in Figure 10. The Ti concentration dependence of grain size of the 321HTB is the same as the Nb concentration dependence of grain size of the 347HTB, where the concentration is expressed in at. pct. The inclusions of Ti- and Nb-carbonitrides act as obstacles for boundary migration during grain growth at solution temperature. Therefore, the higher the Ti and Nb concentration, the finer the grain size. The grain size of the heats ACH and ACJ (31 $\mu$m) of the 321HTB was smaller than that of the heats ACL (63 $\mu$m) and ACN (69 $\mu$m), although the solution temperature of the heats ACH and ACJ [1453 K (1180 °C)] is higher than that of the heats ACL and ACN [1393 K (1120 °C); Table I]. This is due to the higher concentration of Ti in the heats ACH (0.51) and ACJ (0.55 mass pct Ti) than in the heats ACL (0.49) and ACN (0.39 mass pct Ti).

There was no distinct relationship between the time to rupture and grain size in the 304HTB, 316HTB, and 347HTB. This reflects the different precipitation behaviors at grain boundaries between the 321HTB and other steels. In the 321HTB, the precipitation of $M_{23}C_6$ carbides rich in Cr and fine TiC carbides took place mainly at grain boundaries and in the matrix, respectively, in the initial stage of creep.[20,21] The precipitated $M_{23}C_6$ carbides at grain boundaries became dissolved again in favor of further precipitation of thermodynamically more stable TiC and were completely dissolved by 200 to 300 hours at 973 K (700 °C) in all the heats of the present 321HTB. The dissolution of grain boundary $M_{23}C_6$ carbides results in the disappearance of grain

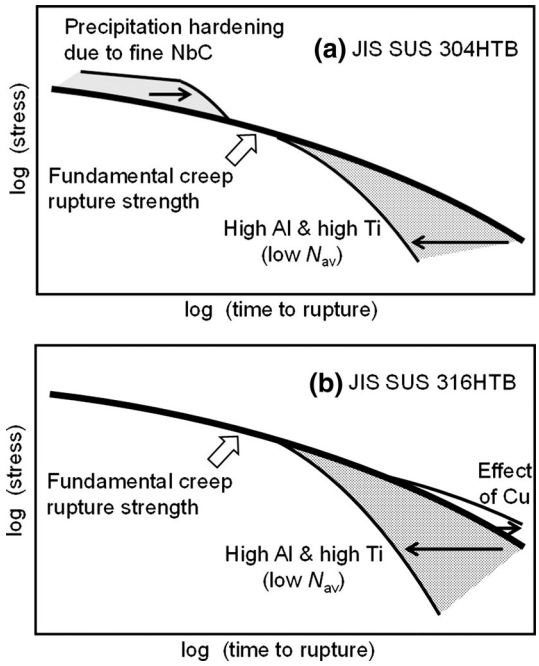


Fig. 16—Schematics of effect of impurities Al, Ti, Nb, and Cu on time to rupture and fundamental creep rupture strength of (*a*) 304HTB and (*b*) 316HTB.

boundary precipitation hardening and hence accelerates grain boundary sliding. This indicates that grain boundaries act as a weak region and that the finer the grains, the shorter the time to rupture.

The precipitation of $M_{23}C_6$ carbides took place at grain boundaries in the 304HTB,[22] 316HTB,[23] and 347HTB[24] in the initial stage of creep, the same as that in the 321HTB.[25] The precipitated $M_{23}C_6$ carbides in the 304HTB and 316HTB were still stable but not disappeared for up to long times during creep, which is quite different from the behavior in the 321HTB. In the 347HTB, fine NbC carbides precipitated mainly in the matrix in the initial stage of creep, in addition to the $M_{23}C_6$ carbide precipitation at grain boundaries. However, the disappearance of precipitated $M_{23}C_6$ carbides in favor of further precipitation of thermodynamically more stable NbC was not observed for most heats of 347HTB steel. The difference in stability of $M_{23}C_6$ carbides during creep between the 321HTB and the 347HTB is because TiC is thermodynamically more stable than NbC, and hence, the decrease in free energy by the change in carbides from $M_{23}C_6$ to TiC is more significant than that from $M_{23}C_6$ to NbC.

The possible mechanisms responsible for the observed heat-to-heat variation in time to rupture of 347HTB relate to (1) impurities boron and phosphorus, which can affect the distributions of $M_{23}C_6$ carbides,; (2) heat treatment condition such solution temperature, which can affect the grain size and soluble Nb concentration; and (3) Nb/C atomic ratio.

### 2. *Effect of impurities boron and phosphorus on heat-to-heat variation in creep life of 347HTB*

The variation in boron concentration among the nine heats, 3 to 27 ppm, explains the heat-to-heat variation in time to rupture of the 347HTB as shown in Figure 11(a). The time to rupture increases with increasing boron concentration and then saturates at about 0.0015 pct (15 ppm) boron. The difference in logarithm of time to rupture ($\Delta\log t_r$) between the high-boron heats with 0.0015 to 0.0027 mass pct boron and low-boron heats with 0.0003 to 0.0004 mass pct boron is evaluated to be about 1.0 for up to about 100,000 hours at 873 K, 923 K, and 973 K (600 °C, 650 °C, and 700 °C) as shown in Figure 11(b), where ($\Delta\log t_r$) = 1.0 means a one order of magnitude increase in creep life. At a high temperature of 1023 K (750 °C), the ($\Delta\log t_r$) decreases with increasing test duration at long times above about 10,000 hours. This suggests that the boron effect becomes less pronounced at long times at a high temperature of 1023 K (750 °C).

The analysis by secondary ion mass spectrometry (SIMS) showed the grain boundary segregation of boron in the heats with boron higher than 12 ppm.[26] The number density of $M_{23}C_6$ carbides along grain boundaries increases with increasing boron concentration as shown in Figure 12(a), indicating that the addition of a small amount of boron enhances fine distributions of $M_{23}C_6$ carbides along grain boundaries in the 347HTB. This enhances the grain boundary precipitation hardening and suppresses the grain boundary displacement or sliding during creep as shown in Figure 12(b), increasing the time to rupture. The grain boundary displacement during creep was measured by observing the displacement of interference fringes and scratch lines at grain boundaries on the specimen surface with plate specimens.[26] The creep test for the plate specimens was carried out in a gas mixture of argon and hydrogen to prevent oxidation of the specimen surface.

There was no distinct relationship between the time to rupture and boron concentration in the 304HTB, 316HTB, and 321HTB steels. The variation in boron concentration among the different heats is smaller in the 304HTB (1 to 18 ppm), 316HTB (5 to 20 ppm), and 321HTB (1 to 10 ppm) than in the 347HTB steel (3 to 27 ppm; Table I). Furthermore, as already described, the heat-to-heat variation in time to rupture of the 304HTB and 316HTB steels is mainly caused by the heat-to-heat variation in available nitrogen concentration, which is strongly influenced by the concentrations of sol Al and Ti. In the 321HTB, the already precipitated $M_{23}C_6$ carbides at grain boundaries in the initial stage of creep become dissolved again in 200 to 300 hours at 973 K (700 °C), and hence, boron has nothing to do with the enhancement of fine $M_{23}C_6$ carbides at grain boundaries.

The addition of 0.1 to 0.3 mass pct phosphorus has a beneficial effect on creep strength of austenitic steels by forming fine $M_{23}C_6$ carbides.[27,28] The effect of phosphorus on the heat-to-heat variation in time to rupture of 347HTB at 973 K (700 °C) and 61 MPa is shown in Figure 13. The phosphorus concentration in the nine heats of 347HTB was rather low at 0.019 to 0.028 mass pct. The phosphorus concentration dependence of time to rupture is split into the two groups: (1) the heats AED, AEE, and AEF containing low boron of 3 to 4 ppm and (2) the other heats containing high

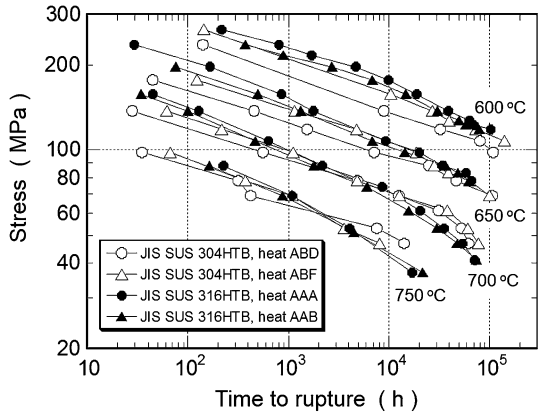


Fig. 17—Fundamental creep rupture strength of 304HTB and 316HTB at 873 K (600 °C) to 1023 K (750 °C).

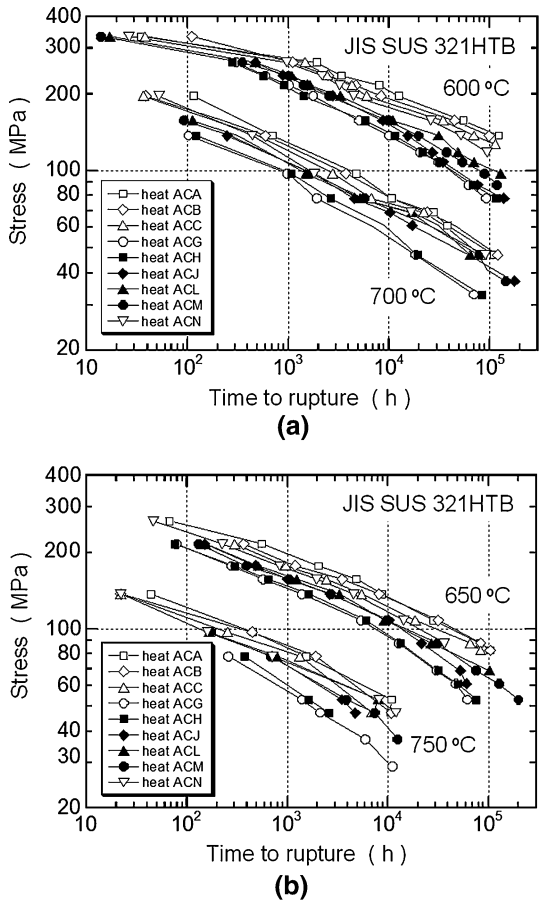


Fig. 18—Fundamental creep rupture strength of 321HTB at (*a*) 873 K (600 °C) and 973 K (700 °C) and (*b*) 923 K (650 °C) and 1023 K (750 °C).

boron of 12 to 27 ppm. There is no distinct relationship between the time to rupture and phosphorus concentration for the two groups because the effect of boron is much stronger than that of phosphorus on the heat-to-heat variation in time to rupture, which is presumably due to the low concentration of phosphorus in the present 347HTB.

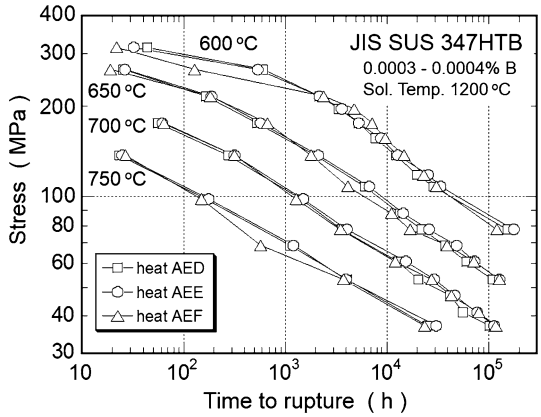


Fig. 19—Fundamental creep rupture strength of 347HTB at 873 K (600 °C) to 1023 K (750 °C).

### 3. *Effect of solution temperature and Nb/C atomic ratio on heat-to-heat variation in creep life of 347HTB*

The present tube materials of 347HTB were hot extruded, cold drawn, solution annealed at 1403 K or 1473 K (1130 °C or 1200 °C) and then quenched in water. Yoshikawa and co-workers reported that the extrapolated 100,000 hours-creep rupture strength of 347HTB at 923 K and 973 K (650 °C and 700 °C) is correlated with the solution temperature.[29] Raising the solution temperature increases the grain size and soluble Nb concentration. Their results suggest that the soluble Nb concentration at solution temperature is a deciding factor for the extrapolated 100,000 hours-creep rupture strength of 347HTB. Soluble Nb causes the precipitation of fine NbC carbides during creep at 873 K to 1023 K (600 °C to 750 °C), which improves the creep strength.

In Figure 1, the time to rupture of heats AED, AEE, and AEF annealed at a higher temperature of 1473 K (1200 °C) is significantly shorter than that of heats AEG, AEH, and AEJ annealed at a lower temperature of 1403 K (1130 °C). It should be noted that the boron concentration is 3 to 4 ppm in the heats AED, AEE, and AEF, which are much lower than that of 18 to 27 ppm in the heats AEG, AEH, and AEJ. The significantly shorter time to rupture of the heats AED, AEE, and AEF than in the heats AEG, AEH, and AEJ is due to the boron effect. The present results indicate that the effect of boron is much stronger than that of solution temperature on the heat-to-heat variation in time to rupture of 347HTB and, hence, that the influence of solution temperature does not explicitly appear.

Minami and Kimura examined the effect of solution temperature from 1273 K to 1573 K (1000 °C to 1300 °C) on the creep rupture strength of 18Cr-10Ni-Nb-Ti stainless steel and showed that the creep rupture strength of the steel at 923 K (650 °C) and 10,000 hours increases linearly with increasing solution temperature.[30] The creep rupture strength of their steel at 923 K (650 °C) and 10,000 hours is 129 and 140 MPa for the solution temperatures of 1403 K (1130 °C), corresponding to the solution temperature of the heats AEG, AEH, and AEJ of the present 347HTB, and 1473 K (1200 °C), which corresponds to the solution

temperature of the heats AED, AEE, and AEF of the present 347HTB, respectively. The difference in creep rupture strength due to the different solution temperatures of 1403 K and 1473 K (1130 °C and 1200 °C) is only 11 MPa at 923 K (650 °C) and 10,000 hours. This is significantly smaller than the difference in creep rupture strength between the weakest and strongest heats of the present 347HTB at 923 K (650 °C) and 10,000 hours; 95 and 165 MPa for the weakest and the strongest heats, respectively, and hence, the difference is 70 MPa. This suggests that the effect of change in solution temperature from 1403 K to 1473 K (1130 °C to 1200 °C) on the creep rupture strength of 347HTB is significantly smaller than the effect of boron described before.

Tanaka and Shinoda reported that $M_{23}C_6$ and NbC carbides played an important role for the creep rupture strength of 18Cr-10Ni-Nb steel containing 0.08 to 0.10 pct carbon and 0.003 to 1.20 pct Nb at 923 K and 973 K (650 °C and 700 °C).[31] They showed that the 10,000 hours-creep rupture strength at 923 K (650 °C) significantly increased at first with increasing Nb/C atomic ratio for up to about Nb/C atomic ratio = 0.1, then gradually increased in the range of Nb/C atomic ratio between about 0.1 and 0.5, and finally decreased after reaching a peak at Nb/C atomic ratio of about 0.5. At 973 K (700 °C); the 10,000 hours-creep rupture strength decreased after reaching a maximum at about Nb/C atomic ratio = 0.1 and was approximately constant above Nb/C atomic ration = 1. They reported that the main strengthening mechanism in creep of the 18Cr-10Ni-Nb steel was due to fine distributions of $M_{23}C_6$ carbides. Near the maximum peak strength, fine $M_{23}C_6$ carbides were homogeneously distributed. However, excess addition of Nb increased the amount of NbC carbides but decreased the $M_{23}C_6$ carbides, resulting in a decrease of creep rupture strength.

The Nb/C atomic ratio of the nine heats of present 347HTB is evaluated to be 1.33 to 2.55, which is much larger than that showing the maximum creep rupture strength reported by Tanaka and Shinoda; Nb/C atomic ratio = 0.5 and 0.1 at 923 K and 973 K (650 °C and 700 °C), respectively. Figure 14 shows the effect of Nb/C atomic ratio on the 10,000 hours-creep rupture strength of the nine heats of present 347HTB at 923 K and 973 K (650 °C and 700 °C), together with the results by Tanaka and Shinoda. The Nb/C atomic ratio dependence of 10,000 hours-creep rupture strength is split into two groups: (1) the heats AED, AEE, and AEF containing low boron of 3 to 4 ppm and (2) the other heats containing high boron of 12 to 27 ppm. The present results on the heats AED, AEE, and AEF containing low boron of 3 to 4 ppm agree well with the results by Tanaka and Shinoda, whereas the creep rupture strength of the other heats is significantly higher than that by Tanaka and Shinoda. This suggests that the large heat-to-heat variation in time to rupture or creep rupture strength in the nine heats of present 347HTB results mainly from the boron effect.

It is concluded that the heat-to-heat variation in time to rupture of the 347HTB is mainly caused by the heat-to-heat variation in boron concentration and that the effect of solution temperature and Nb/C atomic ratio are overlapped with the effect of boron.

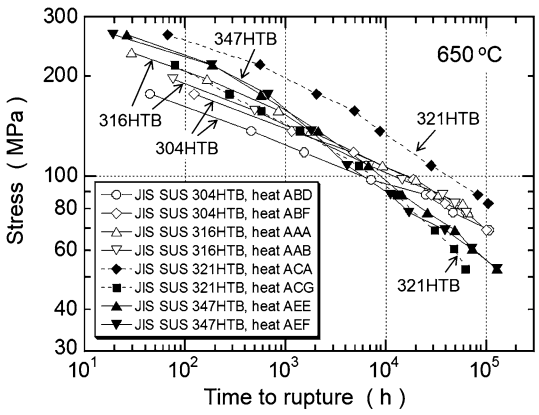


Fig. 20—Fundamental creep rupture strength of 304HTB, 316HTB, 321HTB, and 347HTB at 923 K (650 °C).

### D. *Effect of σ Phase Precipitation on Creep Life*

The precipitation of σ phase takes place at first at grain boundaries and then in the matrix of the present 304HTB,[12] 316HTB,[13] 321HTB,[20,21] and 347HTB[21,26] during creep. In the Metallographic Atlas of NIMS Creep Data Sheets, the time-temperature precipitation (TTP) diagram for σ phase was constructed for the 304HTB,[22] 316HTB,[23] 321HTB,[25] and 347HTB,[24] using the head portions under no stress of crept specimens. Figure 15 compares the TTP diagram for σ phase among the 304HTB, 316HTB, 321HTB, and 347HTB. The initiation time of σ phase precipitation is evaluated to be $1.9 \times 10^3$, $5.5 \times 10^3$, $1.5 \times 10^2$, and $5.5 \times 10^2$ hours for the 304HBT, 316HTB, 321HTB, and 347HTB, respectively, at 973 K (700 °C). The creep fracture mode maps provided by the Metallographic Atlas for the 304HTB, 316HTB, 321HTB, and 347HTB show that at long times above about $3 \times 10^4$, $3 \times 10^4$, $2 \times 10^4$, and $8 \times 10^3$ hours for the 304HBT, 316HTB, 321HTB, and 347HTB, respectively, at 973 K (700 °C), creep voids form at an interface between the σ phase precipitates at grain boundaries and the austenite matrix. At high stresses and short times, where $M_{23}C_6$ carbides precipitate during creep but not σ phase, creep voids form at the interface between $M_{23}C_6$ carbides and the austenite matrix.

Comparing the creep rupture data at 973 K (700 °C) in Figure 1 with the TTP diagram for σ phase in Figure 15, the degradation in creep rupture strength takes place in the 304HTB and 316HTB at long times above about 10,000 hours at 973 K (700 °C), after some amount of σ phase precipitated, because the initiation time of σ phase precipitation is $1.9 \times 10^3$ and $5.5 \times 10^3$ hours for the 304HTB and 316HTB, respectively, at 973 K (700 °C) as shown in Figure 15. However, only the heats with high Al and high Ti exhibit the degradation in the 304HTB and 316HTB,

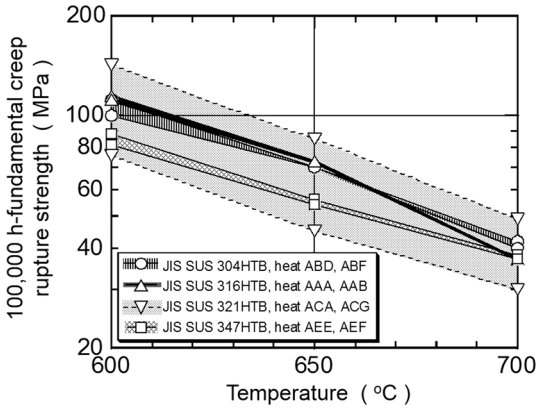


Fig. 21—100,000 hours-fundamental creep rupture strength of 304HTB, 316HTB, 321HTB, and 347HTB, as a function of temperature.

whereas the heats with low Al and low Ti exhibit no degradation for up to long times exceeding 100,000 hours at 973 K (700 °C), as already described. The degradation in the 304HTB and 316HTB is explained by the mechanism of available nitrogen concentration.

The 321HTB and 347HTB steels do not exhibit the degradation in creep rupture strength becoming more significant with time at long times as in the case of the 304HTB and 316HTB, despite the precipitation of $\sigma$ phase in the 321HTB and 347HTB at long times above $1.5 \times 10^2$ and $5.5 \times 10^2$ hours, respectively, at 973 K (700 °C). The large heat-to-heat variation in time to rupture of the 321HTB and 347HTB is explained mainly by the effect of grain size and boron, respectively. Although higher Cr and higher Mo are known to promote the precipitation of $\sigma$ phase, the time to rupture of the 347HTB is substantially the same between the high-Cr heat AEH (18.05 mass pct Cr) and low-Cr heat AEG (17.56 mass pct Cr) and between the high-Mo heat AEJ (0.19 mass pct Mo) and low-Mo heat AEH (0.06 mass pct Mo) at 973 K (700 °C) (Figure 1). These heats contained approximately the same boron concentration. Also in the 321HTB, the time to rupture is substantially the same between the high-Mo heat ACN (0.25 mass pct Mo) and low-Mo heat ACL (0.02 mass pct Mo) at 973 K (700 °C), where these heats exhibit approximately the same grain size. The time to rupture of the high-Cr heat ACH (18.82 mass pct Cr) is a little bit shorter than that of the low-Cr heat ACM (17.71 mass pct Cr). But this may be due to the smaller grain size of heat ACH than of the heat ACM.

The present results indicate that there is no indication showing the promotion of degradation in creep rupture strength by the precipitation of $\sigma$ phase in the present 304HTB, 316HTB, 321HTB, and 347HTB, although $\sigma$ phase particles provide preferential nucleation sites for creep void formation at low stress and long-time conditions. Further investigation will be necessary to make clear the relationship between the creep life and creep void nucleation, growth, and coalescence at $\sigma$ phase particles.

## IV. FUNDAMENTAL CREEP RUPTURE STRENGTH

The observed heat-to-heat variation in time to rupture is caused by the intrinsic effect as well as the extrinsic effect. The extrinsic effect includes the effect of impurities: Al, Ti, nitrogen, and Nb for the 304HTB; Al, Ti, nitrogen, and Cu for the 316HTB; and boron for the 347HTB. The intrinsic effect includes the effect of alloying element Ti for the 321HTB and the effect of solution temperature and Nb/C atomic ratio for the 347HTB, where the concentration of Ti, the solution temperature, and the concentrations of Nb and carbon are specified by JIS. In the following, the fundamental creep rupture strength, which is defined as the creep rupture strength not influenced by impurities, is estimated for the 304HTB, 316HTB, 321HTB, and 347HTB.

### A. *Fundamental Creep Rupture Strength of 304HTB and 316HTB*

Based on the results described, Figure 16 shows schematically the effect of impurities Al, Ti, nitrogen, Nb, and Cu on the time to rupture of 304HTB and 316HTB and the fundamental creep rupture strength not influenced by the impurities. The fundamental creep rupture strength of 304HTB is given by the creep rupture strength of the heats containing very low concentrations of impurities Al, Ti, and Nb, whereas that of 316HTB is the creep rupture strength of the heats containing very low concentrations of impurities Al, Ti, and Cu. The heats ABD and ABF of 304HTB and the heats AAA and AAB of 316HTB contain very low concentrations of these impurities as given in Table I, and hence, these heats provide the fundamental creep rupture strength of 304HTB and 316HTB, respectively. The creep rupture strength of the 304HTB containing high concentrations of sol Al and Ti deviates downward from the fundamental creep rupture strength at long times by the degradation, as already shown in Figure 4. The creep rupture strength of the 304HTB containing a high concentration of Nb is larger than the fundamental creep rupture strength at short times by the precipitation hardening due to fine NbC, but it converges to the fundamental creep rupture strength at long times by the coarsening of NbC, as already shown in Figure 5. Based on the fundamental creep rupture strength, we can understand the creep rupture strength of commercial stocks of 304HTB and 316HTB by taking the effect of impurities into account.

Figure 17 compares the fundamental creep rupture strength between the 304HTB and 316HTB at 873 K to 1023 K (600 °C to 750 °C), where the creep rupture data for the heats ABD and ABF of 304HTB and those for the heats AAA and AAB of 316HTB are shown. At short times less than about 1000 hours, the fundamental creep rupture strength is lower in the 304HTB than in the 316HTB at 873 K to 1023 K (600 °C to 750 °C). At long times, on the other hand, the fundamental creep rupture strength is approximately the same between the two steels at low temperatures of 873 K and 923 K

(600 °C and 650 °C) and at around 100,000 hours, whereas that is a little bit larger in the 304HTB than in the 316HTB at high temperatures of 973 K and 1023 K (700 °C and 750 °C) and above about 10,000 hours. The 100,000 hours-fundamental creep rupture strength of the heats ABD and ABF of 304HTB is evaluated to be 100 to 112, 70 and 40 to 42 MPa at 600 K, 650 K, and 973 K (700 °C), respectively, whereas that of the heats AAA and AAB of 316HTB is evaluated to be 112 to 115, 73 and 37 MPa at 873 K, 923 K, and 973 K (600 °C, 650 °C, and 700 °C), respectively.

### B. *Fundamental Creep Rupture Strength of 321HTB*

The observed large variation in time to rupture among the nine heats of 321HTB is caused by the intrinsic effect due to the heat-to-heat variation in grain size, which is inversely proportional with the concentration of Ti but not caused by the impurity effect. Therefore, all the creep rupture data for the nine heats of 321HTB at 873 K to 1023 K (600 °C to 750 °C) shown in Figure 18 represent the fundamental creep rupture strength of 321HTB from short to long times. The 100,000 hours-fundamental creep rupture strength of the nine heats of 321HTB is evaluated to be 76 to 143, 45 to 85, and 30 to 49 MPa at 873 K, 923 K, and 973 K (600 °C, 650 °C, and 700 °C), respectively.

The concentration of Ti in the nine heats of the present 321HTB, 0.39 to 0.55 mass pct, is located at the high Ti region in the range of JIS specification for Ti in 321HTB, 0.16 to 0.60 mass pct. When the concentration of Ti in commercial materials of 321HTB is lower than the minimum Ti concentration in the present 321HTB, namely, lower than 0.39 mass pct, the creep rupture strength can be larger than the maximum creep rupture strength of the present 321HTB.

### C. *Fundamental Creep Rupture Strength of 347HTB*

The observed heat-to-heat variation in time to rupture of the 347HTB is mainly caused by impurity boron and is a little bit caused by the intrinsic effect due to the change in solution temperature and due to the change in Nb/C atomic ratio. Therefore, the heats AED, AEE, and AEF containing very low boron concentrations of 0.003 to 0.004 mass pct (3 to 4 ppm), practically zero boron, provide the fundamental creep rupture strength of 347HTB. This is shown in Figure 19. The 100,000 hours-fundamental creep rupture strength of the heats AED, AEE, and AEF of 347HTB is evaluated to be 82 to 88, 54 to 56, and 37 to 38 MPa at 873 K, 923 K, and 973 K (600 °C, 650 °C, and 700 °C), respectively.

The heats AED, AEE, and AEF were subjected to solution annealing at 1473 K (1200 °C) as shown in Table I. When commercial stocks of 347HTB are subjected to solution annealing at a low temperature of 1403 K (1130 °C) as in the heats AEG, AEH, and AEJ, which is 70 deg lower than the solution temperature of the heats AED, AEE, and AEF, the fundamental creep rupture strength at 923 K (650 °C) and 10,000 hours can be lowered by 11 MPa, according to the results by Minami and Kimura.[30] On the other hand, the fundamental creep rupture strength of the heats AED, AEE, and AEF at 923 K (650 °C) and 10,000 hours is evaluated to be 90 to 97 MPa, indicating that the variation of creep rupture strength is 7 MPa among the three heats as shown in Figure 19. Therefore, the change in creep rupture strength at 923 K (650 °C) and 10,000 hours by lowering the solution temperature from 1473 K to 1403 K (1200 °C to 1130 °C) is approximately the same as the variation of creep rupture strength among the three heats AED, AEE, and AEF.

The Nb/C atomic ratio of the heats AED, AEE, and AEF is evaluated to be 1.99 to 2.55 as shown in Table I and Figure 14, which is larger than that of the other heats containing high boron of 12 to 27 ppm, Nb/C ratio = 1.33 to 2.12. The decrease in Nb/C atomic ratio from 1.99 to 1.33, corresponding to the decrease in Nb concentration from 0.77 to 0.72 mass pct as shown in Table I, can increase the creep rupture strength at 923 K (650 °C) and 10,000 hours by 7 MPa but no change at 973 K (700 °C) and 10,000 hours, according to the results by Tanaka and Shinoda[31] shown in Figure 14. The increase in creep rupture strength at 923 K (650 °C) and 10,000 hours by a decrease in Nb/C ratio from 1.99 to 1.33 is again approximately the same as the variation of creep rupture strength among the three heats AED, AEE, and AEF. Similar as the situation of Ti in the 321HTB described in the previous section, the concentration of Nb in the nine heats of 347HTB, 0.72 to 0.88 mass pct, is located at the high Nb region in the range of JIS specification for Nb in 347HTB, 0.32 to 1.00 mass pct. When the concentration of Nb in commercial stocks of 347HTB steel is lower than the minimum Nb concentration in the present 347HTB, namely, lower than 0.72 mass pct, the Nb/C atomic ratio is lower than 1.33, and hence, the increase in creep rupture strength at 923 K (650 °C) and 10,000 hours can be larger than 7 MPa as described before. It should be noted that as already described in the Introduction section, the chemical compositions of the present nine heats represent the typical values of most commercial tubes of 347HTB produced in Japan.

It is concluded that the creep rupture data for the three heats AED, AEE, and AEF of 347HTB provide the fundamental creep rupture strength of 347HTB and that the change in creep rupture strength by the change in solution temperature and Nb/C atomic ratio is approximately the same as the variation in creep rupture strength among the three heats.

### D. *Comparison of Fundamental Creep Rupture Strength Among 304HTB, 316HTB, 321HTB, and 347HTB*

Figure 20 compares the fundamental creep rupture strength among the heats ABD and ABF of 304HTB, the heats AAA and AAB of 316HTB, the heats ACA and ACG of 321HTB, and the heats AEE and AEF of 347HTB at 923 K (650 °C). Although all the nine heats of 321HTB provide the fundamental creep rupture strength depending on grain size, only the data for the strongest and weakest heats are shown for simplicity in Figure 20. The fundamental creep rupture strength of

347HTB is higher than that of 304HTB and 316HTB at short times less than 1000 hours, whereas the situation is reversed at long times above 10,000 hours. This is because the slope of stress *vs* time to rupture curves is steeper in the 347HTB than in the 304HTB and 316HTB at long times above 10,000 hours. The slope of stress *vs* time to rupture curves is also steeper in the 321HTB than in the 304HTB and 316HTB, which is similar to the 347HTB. The different behavior between the 304HTB and 316HTB and the 321HTB and 347HTB may be correlated with the different precipitation behavior and the different microstructure evolution during creep. The fine TiC and NbC carbides precipitate in the matrix of the 321HTB and 347HTB, respectively, together with the $M_{23}C_6$ carbides at grain boundaries, in the initial stage of creep, whereas only the $M_{23}C_6$ carbides precipitate in the 304HTB and 316HTB but no TiC nor NbC. The fine TiC and NbC carbides cause the significant precipitation hardening, resulting in the large creep rupture strength at short times. The coarsening of fine TiC and NbC carbides during creep causes a steep decrease in creep rupture strength at long times, resulting in a steeper slope of stress *vs* time to rupture curves.

Figure 21 compares the 100,000 hours-fundamental creep rupture strength among the 304HTB, 321HTB, 321HTB, and 347HTB at 873 K to 973 K (600 °C to 700 °C) as a function of temperature, where only the data for the strongest and weakest heats are shown for the respective steels for simplicity. The 100,000 hours-fundamental creep rupture strength of the 347HTB steel is lower than that of 304HTB and 316HTB at 873 K and 923 K (600 °C and 650 °C) because the slope of stress *vs* time to rupture curves is steeper in the 347HTB than in the 304HTB and 316HTB as shown in Figure 20. At 973 K (700 °C), the difference in 100,000 hours-fundamental creep rupture strength is small among the 304HTB, 316HTB, and 347HTB. The 321HTB exhibits the large variation of 100,000 hours-fundamental creep rupture strength at 873 K to 973 K (600 °C to 700 °C), depending on grain size.

## V. CONCLUSIONS

1. The heat-to-heat variation in time to rupture of the 304HTB and 316HTB is not large at short times less than 1000 hours, but it becomes more significant with increasing test duration at long times above about 10,000 hours at 973 K (700 °C), as shown by about one order of magnitude difference between the strongest and weakest heats at about 100,000 hours. The onset time for increasing the heat-to-heat variation in time to rupture shifts to longer times when the test temperature is decreased. On the other hand, the heat-to-heat variation in time to rupture of the 321HTB and 347HTB is very large of about one order of magnitude difference between the strongest and weakest heats even at a short time of about 100 hours at 973 K (700 °C). Substantially the same magnitude of heat-to-heat variation in time to rupture continues for up to long times exceeding 100,000 hours, which is also typical at low temperatures of 873 K and 923 K (600 °C and 650 °C).
2. The heat-to-heat variation in time to rupture of the 304HTB is mainly caused by the heat-to-heat variation in precipitation hardening due to fine NbC carbides at short times, whereas it is mainly caused by the heat-to-heat variation in available nitrogen concentration, defined as the concentration of nitrogen free from AlN and TiN, at long times. The formation of AlN and TiN during creep reduces the concentration of dissolved nitrogen available for the creep strength. The heat-to-heat variation in time to rupture of the 316HTB is also explained by the concept of available nitrogen concentration and the effect of a small amount of Cu is overlapped at long times.
3. The concept of available nitrogen concentration cannot be applied to the 321HTB and 347HTB, which are alloyed with 0.39 to 0.55 mass pct Ti and 0.72 to 0.88 mass pct Nb, respectively, because most nitrogen atoms form inclusions of Ti- and Nb-nitrides at a high temperature and, hence, dissolved nitrogen is scarcely present in these steels after solution treatment. The heat-to-heat variation in time to rupture of the 321HTB is caused by the heat-to-heat variation in grain size, which is inversely proportional with the concentration of Ti.
4. The heat-to-heat variation in time to rupture of the 347HTB is mainly explained by impurity boron. The effect of impurity phosphorus, solution temperature, and Nb/C atomic ratio does not explicitly appear because the effect of boron is much stronger than that of these factors in the 347HTB. Boron enhances fine distributions of $M_{23}C_6$ carbides along grain boundaries, which enhances the grain boundary precipitation hardening, increasing the time to rupture. The effect of boron becomes less pronounced with increasing test duration at long times above about 10,000 hours at a high temperature of 1023 K (750 °C).
5. The fundamental creep rupture strength, which is defined as the creep rupture strength not influenced by impurities, is estimated for the respective steels. The fundamental creep rupture strength of 304HTB is given by the creep rupture strength of the heats containing very low concentrations of impurities Al, Ti, and Nb, whereas that of 316HTB is the creep rupture strength of the heats containing very low concentrations of impurities Al, Ti, and Cu. All the creep rupture data for the nine heats of 321HTB represent the fundamental creep rupture strength depending on grain size, which is inversely proportional with the concentration of Ti. The fundamental creep rupture strength of 347HTB is given by the creep rupture strength of the heats containing a very low concentration of impurity boron.
6. The 100,000 hours-fundamental creep rupture strength of the 347HTB steel is lower than that of 304HTB and 316HTB at 873 K and 923 K (600 °C and 650 °C) because the slope of stress *vs* time to rupture curves is steeper in the 347HTB than in the

304HTB and 316HTB. The 100,000 hours-fundamental creep rupture strength of the 321HTB exhibits the large variation at 873 K to 973 K (600 °C to 700 °C) depending on the variation in grain size.

## ACKNOWLEDGMENT

The present author would like to thank Dr. H. Tanaka and Mr. M. Murata at NIMS for their observations of microstructure evolution in the present steels during creep.

## REFERENCES

1. Series of NIMS (formerly NRIM) Creep Data Sheets No. 1-55. Tokyo, Tsukuba, National Institute for Materials Science, 2015.
2. F. Abe: *Int. J. Pressure Vessels Piping*, 2008, vol. 85, pp. 99–107.
3. NIMS Creep Data Sheets No. 3B. Tokyo, Tsukuba, Japan, National Institute for Materials Science, 1986.
4. NIMS Creep Data Sheets, No. 43A, Tokyo, Tsukuba, Japan, National Institute fort Materials Science, 2014.
5. NIMS Creep Data Sheets, No. 4B, Tokyo, Tsukuba, Japan, National Institute fort Materials Science, 1986.
6. F. Abe, H. Tanaka, M. Murata, H. Irie and K. Yagi: *Proc. of 4th Japan-China Bilateral Symp. on High Temp. Strength of Mater.,* June 2001, Tsukuba, Japan, pp. 83–88.
7. H. Miyazaki, H. Tanaka, M. Murata, and F. Abe: *J. Jpn Inst. Metals*, 2002, vol. 66, pp. 1278–86.
8. F. Abe: *Int. J. Pressure Vessels Piping*, 2010, vol. 87, pp. 310–18.
9. S. J. Brett, J. S. Bates and R. C. Thomson: *Proc. of Fourth International Conference on Advances in Materials Technology for Fossil Power Plants*, October 2004, Hilton Head, North Carolina, USA, pp. 202–16.
10. SJ Brett: *Energy Mater*., 2007, vol. 2, pp. 117–21.
11. H. Naoi, M. Ohgami, X. Liu, and T. Fujita: *Metall. Mater. Trans. A*, 1997, vol. 28A, pp. 1195–1203.
12. N. Shinya, J. Kyono, H. Tanaka, M. Murata, and S. Yokoi: *Tetsu-To-Hagane*, 1983, vol. 69, pp. 1668–75.
13. N. Shinya, H. Tanaka, M. Murata, J. Kyono, and S. Yokoi: *Tetsu-To-Hagane*, 1985, vol. 71, pp. 114–20.
14. NIMS Creep Data Sheets, No. 6B, Tokyo, Tsukuba, Japan, National Institute fort Materials Science, 2000.
15. NIMS Creep Data Sheets, No. 5B, Tokyo, Tsukuba, Japan, National Institute fort Materials Science, 1987.
16. NIMS Creep Data Sheets, No. 28B, Tokyo, Tsukuba, Japan, National Institute fort Materials Science, 2001.
17. R.K. Winge, V.A. Fassel, V.J. Peterson, and M.A. Floyd: *Inductively Coupled Plasma-Atomic Emission Spectroscopy*, Elsevier, Amsterdam, 1985, pp. 1–25.
18. JIS G 0551: *Steels – Micrographic Determination of the Apparent Grain Size*, Japanese Industrial Standard, 2013.
19. ASTM E112: *Standard Test Methods for Determining Average Grain Size*, Annual Book of ASTM Standards, 2005.
20. H. Tanaka, M. Murata, and N. Shinya: *Tetsu-To-Hagane*, 1992, vol. 78, pp. 934–40.
21. H. Tanaka, M. Murata, F. Abe, and K. Yagi: *Mater. Sci. Eng*., 1997, vols. A234–236, pp. 1049–52.
22. Metallographic Atlas of Long-Term Crept Materials, M-1, Tokyo, Tsukuba, National Institute fort Materials Science, 1999.
23. Metallographic Atlas of Long-Term Crept Materials, M-2, Tokyo, Tsukuba, National Institute fort Materials Science, 2003.
24. Metallographic Atlas of Long-Term Crept Materials, M-5, Tokyo, Tsukuba, National Institute fort Materials Science, 2006.
25. Metallographic Atlas of Long-Term Crept Materials, M-3, Tokyo, Tsukuba, National Institute fort Materials Science, 2004.
26. H. Tanaka, M. Murata, F. Abe, and K. Yagi: *Tetsu-to-Hagane*, 1997, vol. 83, pp. 72–77.
27. F.H. Froes, M.G.H. Wells, and B.R. Banerjee: *Met. Sci. J*., 1968, vol. 2, pp. 232–34.
28. T. Matsuo, T. Shinoda, and R. Tanaka: *Tetsu-to-Hagane*, 1973, vol. 59, pp. 907–18.
29. K. Yoshikawa, H. Fujikawa, H. Teranishi, H. Yuzawa, and M. Kubota: *Thermal Nucl. Power*, 1985, vol. 36, pp. 1325–39.
30. Y. Minami and H. Kimura: *Trans. ISIJ*, 1987, vol. 27, pp. 299–301.
31. R. Tanaka and T. Shinoda: *J. Soc. Mater. Sci. Jpn*., 1972, vol. 21, pp. 198–203.